Magnetic dipole moments of ^{57,58,59}Cu

T. E. Cocolios,[1] A. N. Andreyev,[1] B. Bastin,[1] N. Bree,[1] J. Büscher,[1] J. Elseviers,[1] J. Gentens,[1] M. Huyse,[1] Yu. Kudryavtsev,[1] D. Pauwels,[1] T. Sonoda,[1,2] P. Van den Bergh,[1] and P. Van Duppen[1]

[1]*Instituut voor Kern- en Stralingsfysica, K.U. Leuven, B-3001 Leuven, Belgium*

[2]*RIKEN, Wako, Saitama 305-0198, Japan*

(Received 22 October 2009; published 28 January 2010)

In-gas-cell laser spectroscopy of the isotopes ^{57,58,59,63,65}Cu has been performed at the LISOL facility using the 244.164-nm optical transition from the atomic ground state of copper. A detailed discussion on the hyperfine structure of ^{63}Cu is presented. The magnetic dipole moments of the isotopes ^{57,58,59,65}Cu are extracted based on that of ^{63}Cu. The new value $\mu = +0.479(13)\mu_N$ is proposed for ^{58}Cu, consistent with that of a $\pi p_{3/2} \otimes \nu p_{3/2}$ ground-state configuration. Spin assignments for the radioactive isotopes ^{57,58,59}Cu are confirmed. The isotope shifts between the different isotopes are also given and discussed.

DOI: 10.1103/PhysRevC.81.014314 PACS number(s): 21.10.Ky, 27.40.+z, 27.50.+e, 42.62.Fi

I. INTRODUCTION

Magic numbers are the cornerstones of the shell model of the nucleus. While those are well established for the stable nuclei, their persistence away from the valley of β stability is questioned. The magic number 28 is the first to arise from the addition of the spin-orbit term to the nuclear potential. This is why nuclei in the vicinity of $N = 28$ [1,2] and of nickel ($Z = 28$) [3,4] are under current investigation to probe the magic nature of these shell closures far from stability. With $N = Z = 28$, ^{56}Ni is expected to be doubly magic. Indeed, it presents a high excitation energy for the 2_1^+ excited state in comparison to the other nickel isotopes [3] and a sudden change in the two-neutron and two-proton separation energies [5]. However, the evolution of the $B(E2)$ does not drop as sharply as expected for a doubly magic nucleus [6]. Moreover, the properties of the neighboring nuclei cannot be explained by simply coupling particles and/or holes to the ^{56}Ni core but require excitations of this core [7,8].

The study of the nuclear magnetic dipole moments in the vicinity of that nucleus is essential to further the understanding of the different processes at play. Of special interest is the copper isotopic chain ($Z = 29$), which consists, in the frame of the shell model, of a single proton added to the nickel core. For the odd-A copper isotopes, the magnetic dipole moment is then governed by the single proton while in the case of the even-A odd-odd copper isotopes, the coupling of the proton and a neutron should be responsible for the magnetic dipole moment. Extensive studies on the copper isotopic chain have therefore been performed [9–14] and are still current [15,16].

The nuclear dipole moments of the odd-A copper isotopes have been found to depart strongly from the Schmidt value $+3.79\mu_N$. This difference increases significantly while going from $N = 40$ down to $N = 30$ [11] but the trend breaks for the $N = 28$ isotope ^{57}Cu as it rises to a higher value, yet not sufficiently to be explained by the shell-model calculations [12]. This discrepancy pointed toward a larger breaking of the core than anticipated. This last isotope was studied using the β-NMR technique at a fragmentation facility but the resonance, seen in Fig. 1 of Ref. [12], was of limited quality. Further confirmation of this result using a different method was therefore necessary, e.g., via in-source laser spectroscopy [13]. The new result reported in Ref. [15] disagrees with the literature value and is much closer to the shell-model calculations [8,13]. In this article, more details on the analysis of the results reported in Ref. [15] will be given, together with new data obtained for the isotope ^{58}Cu.

Using laser spectroscopy, it is possible to study the influence of the nucleus on atomic transitions by means of laser radiation. Through the interaction between the electron angular momentum and the nucleus electromagnetic moments, the degeneracy of the atomic levels can be lifted, giving rise to a new set of states, the hyperfine levels, with quantum number F such that

$$|I - J| \leqslant F \leqslant I + J, \tag{1}$$

where I is the nuclear spin and J is the electron angular momentum. The change in energy ΔE of a given hyperfine level with respect to the degenerate energy level is then given by

$$\Delta E = \frac{A_{\mathrm{hf}}}{2} \times K + \frac{B_{\mathrm{hf}}}{2} \times \frac{3K(K+1) - 2I(I+1)2J(J+1)}{2I(2I-1)2J(2J-1)}, \tag{2}$$

where A_{hf} and B_{hf} are called the dipole and quadrupole hyperfine parameters, respectively, and $K = F(F+1) - I(I+1) - J(J+1)$. The magnetic dipole moment μ enters in the dipole hyperfine parameter

$$A_{\mathrm{hf}} = \frac{\mu \times H_0}{IJ}. \tag{3}$$

H_0 is the magnetic field at the position of the nucleus generated by the electron motion. This parameter is specific to the transition studied and remains independent of the isotope. One can then measure the different transitions, deduce the hyperfine parameters and, in the absence of hyperfine anomaly, extract the moment of one isotope given that of another isotope [17]. The specific case of copper will be discussed in the section on analysis and discussion.

For the copper isotopes, high-precision in-flight laser spectroscopy has been performed down to the $N = 32$ isotope ^{61}Cu [18]. The study of the more exotic nuclei on the neutron-deficient side requires higher sensitivity to cope with the reduced beam intensities. In-source spectroscopy is ideally suited for this type of sensitive measurement [19]. The hot cavity target and ion source, however, can suffer from large decay losses due to the diffusion and effusion processes from the target to the atomizer [20]. As a consequence, the short-lived $T_{1/2} = 199$ ms isotope ^{57}Cu is presently beyond reach of the hot-target facilities [13].

Gas catchers, on the other hand, suffer less from such limitations as the nuclear reaction products recoil directly out of the target and can be used for laser spectroscopy studies [21]. We report here on such study on the stable isotopes ^{63,65}Cu and on the neutron-deficient isotopes ^{57,58,59}Cu. We detail the systematic study of the stable ^{63}Cu, which was used to assert the reliability of the in-gas-cell laser spectroscopy technique, used for the first time at an online mass separator. The hyperfine structure of the odd-A isotopes ^{57,59,63,65}Cu as well as that of ^{58}Cu are analysed and presented. The magnetic dipole moments are extracted and that of ^{58}Cu is discussed. The spin assignments for those isotopes are confirmed. Finally, the isotope shifts are extracted and the possibility of determining changes in the mean-square charge radius is discussed.

II. EXPERIMENTAL DETAILS

A. Production and spectroscopy

The experiment was performed online at the Leuven Isotope Separator On-Line (LISOL) facility in the Centre de Recherche du Cyclotron (Cyclotron Research Center, CRC), Louvain-La-Neuve (Belgium). The CYCLONE110 cyclotron provided beams of ^{3}He (25 MeV, 2 μA) and protons (30 MeV, 2 μA). Those beams impinged on a thin (thickness 5 μm) natural nickel target (68% ^{58}Ni, 26% ^{60}Ni). The isotopes of interest are produced in the dual chamber laser ion source [22]. The radioactive isotopes $^{57-59}$Cu are produced from the nuclear reactions ^{58}Ni$(p,2n)^{57}$Cu, ^{58}Ni$(p,n)^{58}$Cu, ^{60}Ni$(p,3n)^{58}$Cu, ^{60}Ni$(p,2n)^{59}$Cu, and ^{58}Ni$(^3$He$,pn)^{59}$Cu. Finally, the stable isotopes ^{63,65}Cu are produced from the resistive heating of a natural copper filament.

The recoils are thermalized and neutralized in 130 mbar of argon. The atoms are transported from the stopping chamber to the ionization chamber by the gas flow. In the latter volume, they are irradiated by laser light to be ionized to a Cu^+ state in a two-step two-color resonant process [22,23] shown in Fig. 1. One of the valence electrons is brought from the $3d^{10}4s\ ^2S_{1/2}$ ground state to the $3d^9 4s4p\ ^4P^\circ_{1/2}$ excited state at 40943.73 cm^{-1} via a transition at 244.164 nm; this electron is further excited to the $3d^9 4s5s\ ^4D_{3/2}$ autoionizing state at 63584.57 cm^{-1} beyond the ionization potential.

The ions leave the gas cell through a 1-mm exit hole in the supersonic jet made by the argon buffer gas. They are caught by the pseudopotential of a radiofrequency sextupole ion guide, accelerated to an energy of 40 keV and finally separated according to their mass-to-charge ratio in a dipole magnet.

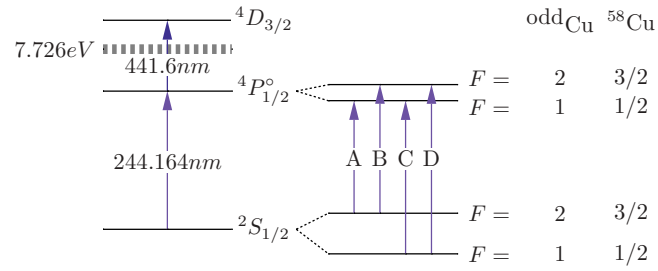

FIG. 1. (Color online) Laser ionization scheme of copper used in this work. The right part shows the hyperfine splittings and transitions. The thick dashed line is the ionization potential. The labels A,B,C,D will be used to label the different transitions in Figs. 2 and 6.

The stable isotopes ^{63,65}Cu are counted in a secondary electron multiplier placed after the collector chamber of the mass separator. The radioactive isotopes $^{57-59}$Cu are implanted on a mylar tape and counted via their respective β decay using three plastic detectors (efficiency 50% [24]). The mylar tape is frequently moved to remove the longer-lived activity and present a fresh sample for further measurement. A feature of the dipole magnet is to allow the simultaneous detection of multiple beams. During the online study of the radioactive nuclei, a stable isotope ion beam is measured at the same time to monitor the behavior of the ion source and to minimize systematic effects; ^{63}Cu was used as a reference for ^{57,58}Cu while ^{65}Cu was used for ^{59}Cu.

The laser system has been thoroughly described in Ref. [25]. It consists of two tuneable dye lasers pumped by two XeCl excimer lasers. The maximum repetition rate is 200 Hz. The first-step dye laser is frequency doubled to reach the UV transition at 244.164 nm. The energy reached per pulse for this transition is 100 μJ; the energy reached per pulse for the second step is 1 mJ. The laser spectroscopy is performed by scanning the laser frequency of the first step of the ionization process from the $^2S_{1/2}$ state to the $^4P^\circ_{1/2}$ state across a range of 35 GHz and by observing the number of ions produced as a function of the applied frequency. The linewidth of this laser is minimized by using an etalon in the oscillator. A full width at half maximum of $\Delta \approx 1.6$ GHz is reached for the second harmonic UV beam. The laser frequency at each step is recorded with a Lambdameter LM-007. Typical resonance spectra can be seen in Fig. 2.

B. Systematic study of ^{63}Cu

In order to assert the reliability of the in-gas-cell laser spectroscopy technique, used for the first time at an online mass separator, several effects have been systematically studied. In this section, we report on our findings regarding the effect of the gas cell pressure, the influence of the ionization transition and the systematic fluctuations of the wavemeter. It is concluded that no systematic uncertainties have to be

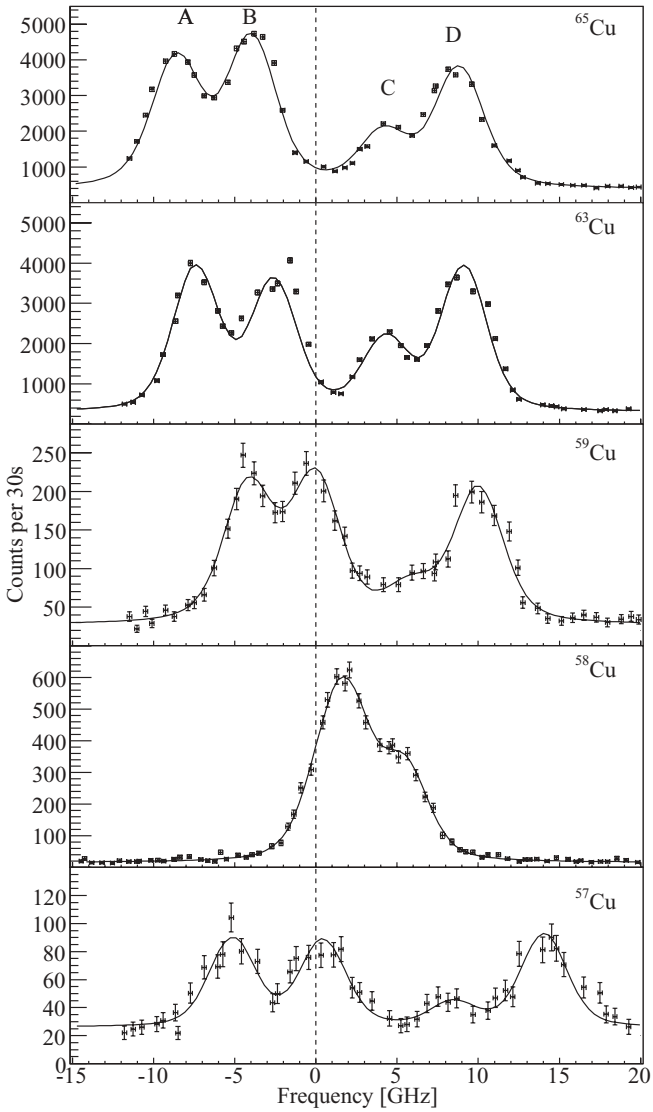

FIG. 2. Typical examples of the single hyperfine spectra of ^{57,58,59,63,65}Cu (bottom to top). Each point is sampled for 30 seconds. ^{57}Cu and ^{63}Cu are measured simultaneously; so are ^{58}Cu and ^{63}Cu or ^{59}Cu and ^{65}Cu. The frequency axis is centered at the center of gravity of ^{63}Cu. A,B,C,D are labels for each hyperfine transition as described in Fig. 1.

added by any of these effects. The fluctuations in the relative intensities of each component is also discussed.

1. *Pressure effects*

A systematic study of the effects of the pressure on the laser spectra has been performed. The gas cell pressure is the main source of broadening of the line, as discussed in Ref. [21]. A pressure broadening of 5.4 MHz mbar^{-1} has been measured, as well as an overal pressure shift of -1.9 MHz mbar^{-1}. The hyperfine structure of ^{63}Cu was measured at different pressures ranging from 60 to 250 mbar. The extracted hyperfine parameter for the atomic ground state is shown as a function of the pressure in Fig. 3. No influence of the pressure can be seen on this parameter.

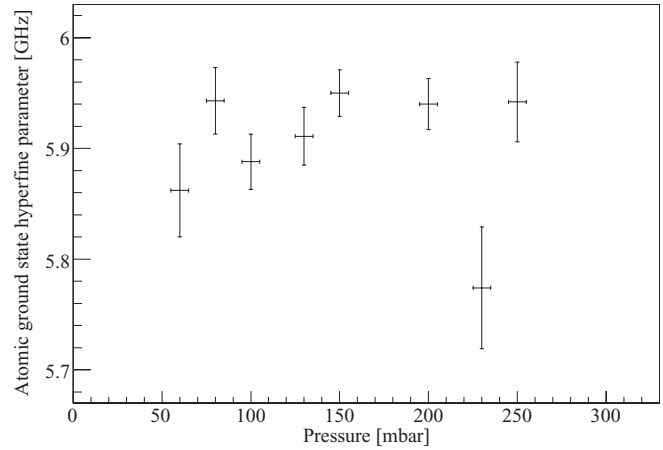

FIG. 3. Effect of the pressure on the hyperfine parameter $A_{\mathrm{hs:gs}}$ of the atomic ground state of ^{63}Cu.

All the peaks are therefore shifted by a similar amount. A similar effect is expected on the isotope shift between two isotopes.

2. *Influence of the ionization transition*

Laser scanning of the ionization transition has been performed from each hyperfine sub-level of the atomic excited state by setting the first-transition laser to excite the valence electron into either the $F = 1$ or the $F = 2$ level. The scans of the ionizing transition are shown in Fig. 4.

The resonance spectrum to the autoionizing level is the same for both hyperfine levels. Its width is above 150 GHz and therefore covers the large splitting (20 GHz) of the excited state completely in spite of the smaller laser bandwidth (5 GHz). The position of the maximum is the same for both cases within our accuracy and no systematic effect can be attributed to the ionizing transition. Finally, hyperfine spectra of ^{63}Cu were acquired at different frequencies for

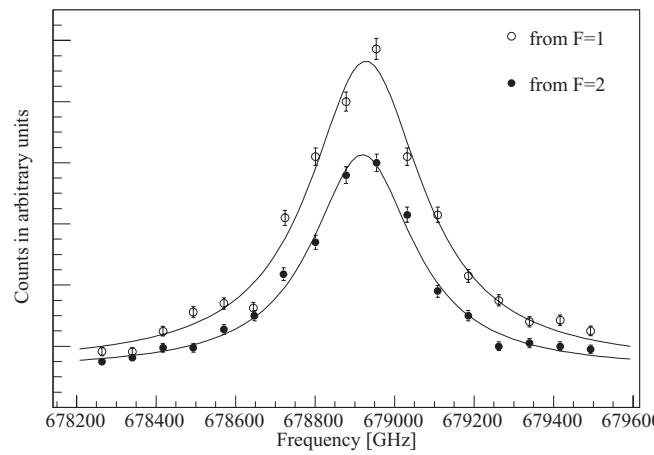

FIG. 4. Spectroscopy of the ionization transition in ^{63}Cu while populating either the $F = 1$ (open circles) or the $F = 2$ (full circles) hyperfine level of the intermediate excited state.

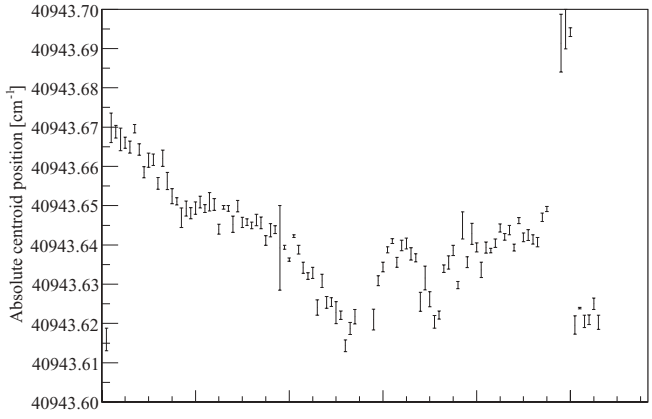

FIG. 5. Evolution of the center of gravity of ^{63}Cu in the course of the experiment. The x axis represents the consequent order of the different runs, spanning a time of 7 days.

the ionizing transition. No changes in the structure could be observed.

3. *Systematic fluctuations*

The online experiment was performed over a period of seven days. Many beam and environmental parameters fluctuate on an hourly or daily basis, possibly affecting the result. It was not possible to monitor all of those parameters and only cumulative effects can be seen on the spectra.

First, the absolute laser frequency is measured for each step. The analysis of the hyperfine spectra returns therefore the absolute transition frequency. Figure 5 shows the evolution of that absolute transition frequency for ^{63}Cu in the course of the experiment. Fluctuations of up to 1 GHz per day have been observed. The fluctuations are, however, occuring over a time scale much larger than the scan time and the reading is considered accurate within a single scan. This drift is due to thermal expansion of mechanical pieces in the laser laboratory as the temperature of this room changes. Note, however, that the hyperfine parameter is extracted from the difference in the position of the different peaks, which is independent of the absolute peak position. Similarly, the isotope shift between any two isotopes is the difference in absolute frequency and this systematic shift cancels out in the analysis.

Large fluctuations of the relative intensities of the hyperfine peaks have also been observed, as shown in Fig. 6. As a consequence, the relative intensities cannot be relied on for the determination of nuclear spins. The relative intensity of the different components in in-source laser ionization spectroscopy has been described thoroughly in Ref. [26]. The lack of information on the ionizing transition used in this experiment does not allow for the full calculation to be performed. Moreover, fluctuations of the gas pressure and of the chamber temperature can affect the population distribution. Nevertheless, the peak labeled C in Fig. 2 is systematically smaller than the other three and can therefore be attributed to the $F = 1 \rightarrow 1$ transition. Based on this, one can still determine the sign of the hyperfine parameters and, hence, that of the moments.

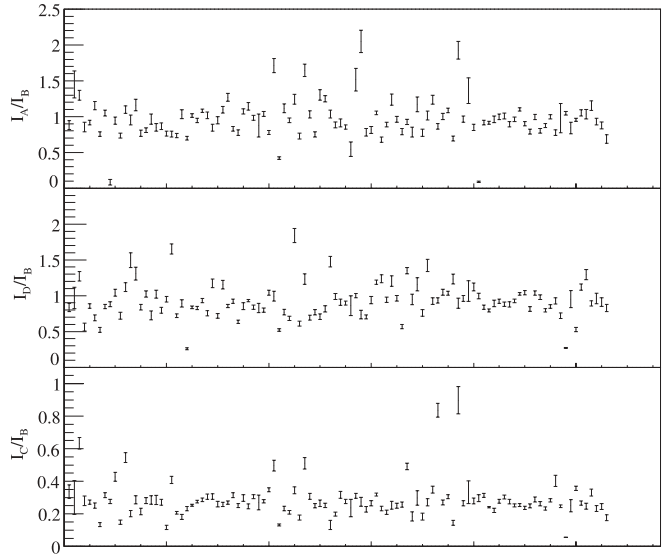

FIG. 6. Evolution of the relative intensity of the C (bottom), D (middle), and A (top) transitions of the hyperfine spectrum of ^{63}Cu with respect to the B transition in the course of the experiment. The labels are given according to Fig. 1 The x axis represents the consequent order of the different runs, spanning a time of 7 days.

III. ANALYSIS AND DISCUSSION

A. Odd-*A* isotopes

1. *Data analysis*

The laser spectroscopy is performed on a $J = \frac{1}{2} \rightarrow \frac{1}{2}$ atomic transition. With the chosen transition, for any nuclear spin $I > \frac{1}{2}$, four transitions are expected. If $I = 0$, no hyperfine structure can be seen; if $I = \frac{1}{2}$, only three transitions can occur as $F = 0 \rightarrow 0$ is a forbidden transition. The appearance of four peaks in the hyperfine spectra of ^{57,59,63,65}Cu is a confirmation that the spin of those odd-A isotopes is at least $\frac{3}{2}$. For the rest of the work, the known spin $I = \frac{3}{2}$ for ^{57,59,63,65}Cu is used.

As seen in Eq. (2), if either $I = \frac{1}{2}$ or $J = \frac{1}{2}$, the scaling factor in front of the hyperfine parameter B diverges and no quadrupole moment can be measured. Thus, the study can only give information on the magnetic dipole moment μ. The position of each peak (ν_i) is then given by a linear combination of the center of gravity of the transition, ν_0, and the hyperfine parameters of the atomic ground state, $A_{\text{hf:gs}}$, and the excited state, $A_{\text{hf:es}}$:

$$\nu_i = \nu_0 + \frac{A_{\text{hf:es}}}{2} \times K_{\text{i:es}} - \frac{A_{\text{hf:gs}}}{2} \times K_{\text{i:gs}}, \tag{4}$$

where $K_i = -\frac{5}{2}$ or $K_i = \frac{3}{2}$, depending on the hyperfine levels. The position of the four peaks is therefore defined by three parameters only.

In each run, two isotopes are always measured in parallel, namely ^{57,63}Cu or ^{59,65}Cu. For each run, the line shape, thoroughly described in Ref. [21], is determined from the

TABLE I. Measured hyperfine parameters $A_{\text{hf:exp}}$ for the atomic ground (gs) and excited (es) states (except for ^{58}Cu), their ratio, and the deduced moments μ_{exp} using ^{63}Cu as the reference isotope. The literature values $A_{\text{hf:lit:gs}}$ [13,27], μ_{lit} [11,12,28,29] and theoretical calculations using GXPF1 [8,14] are given for comparison; the atomic excited hyperfine parameter has no prior measurement.

A	I	$A_{\text{hf:exp:gs}}$ (GHz)	$A_{\text{hf:lit:gs}}$ (GHz)	$A_{\text{hf:exp:es}}$ (GHz)	$\frac{A_{\text{hf:exp:es}}}{A_{\text{hf:exp:gs}}}$	μ_{exp} (μ_N)	μ_{lit} (μ_N)	μ_{GXPF1} (μ_N)
57	$3/2^-$	6.785(15)		2.834(16)	0.418(3)	+2.582(7)	2.00(5)	2.489
58	1^+	1.891(52)	2.11(57)			+0.479(13)	+0.52(8)	0.600
59	$3/2^-$	5.033(10)	4.87(9)	2.069(8)	0.411(2)	+1.910(4)	+1.891(9)	1.886
63	$3/2^-$	5.858(10)	5.866908706(20)	2.432(8)	0.415(2)		2.2273602(13)	2.251
65	$3/2^-$	6.288(17)	6.284389972(60)	2.588(15)	0.412(3)	+2.387(7)	2.3818(3)	2.398

stable spectrum and applied to the radioactive isotope. The typical line width is 3.5 GHz. As mentioned previously, the relative intensities cannot be relied on and the amplitude of each component is left unconstrained.

During the experiment, 106 independent measurements have been performed on ^{63}Cu, 68 on ^{57}Cu, and 34 on ^{59,65}Cu. The extracted hyperfine parameters $A_{\text{hf:gs}}$ and $A_{\text{hf:es}}$ for the atomic ground and excited states, respectively, are shown in Fig. 7. As discussed in the study of ^{63}Cu, the hyperfine parameters do not suffer from any drift and accurate averages can be extracted. The averages are given in Ref. [15] and in Table I.

The correlation between the hyperfine parameters of each atomic level for a given isotope is also investigated. This investigation is shown in Fig. 8. The two hyperfine parameters for each isotope are distributed in a circular scatter and are not correlated in the data analysis. They therefore offer two independent measurements of the magnetic dipole moment. The ratio of the two parameters, represented by the line accross Fig. 8 and given in Table I, are constant from one isotope to the next, as expected in the absence of hyperfine anomaly. Indeed, this effect is expected to be too small to be observed with the limited resolution of the in-source technique [30]. The average of the ratio is 0.414(2).

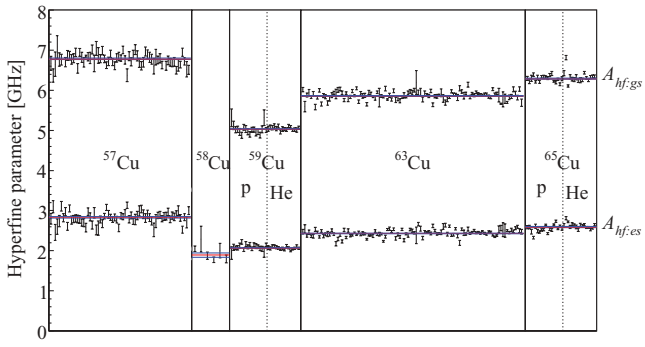

FIG. 7. (Color online) Systematic extracted hyperfine parameters A_{hf} of ^{57,58,59,63,65}Cu for the atomic ground state ($A_{\text{hf:gs}}$) and of ^{57,59,63,65}Cu for the atomic excited state ($A_{\text{hf:es}}$). In the case of ^{59,65}Cu, data using both reactions are presented, identified by the primary beam used, proton (p), or ^{3}He (He), respectively. The x axis represents the succession of experimental runs. The solid lines are the averages through the points.

2. *Magnetic dipole moments*

Based on Eq. (3), the magnetic dipole moments are extracted for each atomic level separately, relative to ^{63}Cu, according to the following

$$\mu = \mu_{63} \times \frac{A_{\text{hf}}}{A_{\text{hf:63}}} \times \frac{I}{I_{63}}. \tag{5}$$

The calculated moments are then averaged within each isotope for the two atomic levels. The results, using a spin $I = \frac{3}{2}$ for each isotope, are given in Table I. A spin assignment $I = \frac{5}{2}$ for ^{57,59}Cu has also been investigated and yielded unphysical moments, larger than the Schmidt limit. This further confirms the spin assignment $I = \frac{3}{2}$.

The implication of the measurement of those dipole moments has been discussed in Ref. [15]. The measured dipole moments for ^{59,65}Cu are in good agreement with the previous measurements while that of ^{57}Cu[$\mu = +2.582(7)\mu_N$] is in disagreement with that presented in Ref. [12] [$\mu = 2.00(5)\mu_N$]. Since our measurement has been repeated many times and since the systematic effects have been thoroughly investigated, the result in Ref. [12] is strongly questioned. Finally, the magnetic moments of the neutron-deficient copper isotopes are very well reproduced by the shell-model calculation using the FPD6 interaction [31] or the GXPF1 interaction [8,14].

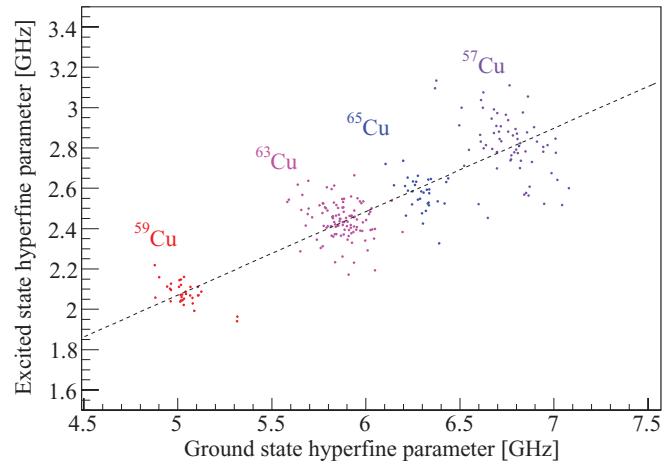

FIG. 8. (Color online) Distribution of the atomic excited state hyperfine parameter $A_{\text{hf:es}}$ as a function of that of the atomic ground state $A_{\text{hf:gs}}$ for ^{57,59,63,65}Cu. The dotted line is the average of the ratio over the four isotopes.

B. Odd-odd isotope ^{58}Cu

1. Data analysis

Six measurements of the hyperfine structure of ^{58}Cu have been performed. Due to its small magnetic dipole moment, the hyperfine structure of ^{58}Cu is collapsed. A structure can, however, be seen, confirming that the spin is not 0. A spin $I = 1$ is used. The four peaks cannot be resolved, unlike in the case of the odd-A isotopes (see Fig. 2). Further constraints are therefore required in order to fit the hyperfine spectrum properly, for example, using a similar approach to that described in Ref. [13].

In order to reduce the number of free parameters, the ratio of the two hyperfine parameters is used:

$$A_{\text{hf:es}} = 0.414 \times A_{\text{hf:gs}}. \tag{6}$$

As a result, only one parameter can be extracted from the analysis of the hyperfine spectrum and the precision on the determination of the magnetic dipole moment is less than in the odd-A case. The difference with the work from Ref. [13] is that the calculated relative intensities cannot be relied on, as discussed before on ^{63}Cu. The only limit is that no peak can disappear totally from the hyperfine spectrum.

The spectra are then fitted similarly to those of ^{57}Cu, using four Voigt profiles with the line-shape parameters from ^{63}Cu, for which the position is determined by combining Eqs. (4) and (6). The systematic extracted values are shown in Fig. 7. The average is given in Table I. In spite of the limited resolution, the hyperfine parameter of the atomic ground state is found to be $A_{\text{hf:gs}} = +1.891(52)$ GHz, in agreement with the hot cavity result 2.11(57) GHz but with 10 times higher precision.

2. Magnetic dipole moment

Similarly to the odd-A copper isotopes, the magnetic dipole moment of ^{58}Cu can be extracted based on that of ^{63}Cu.

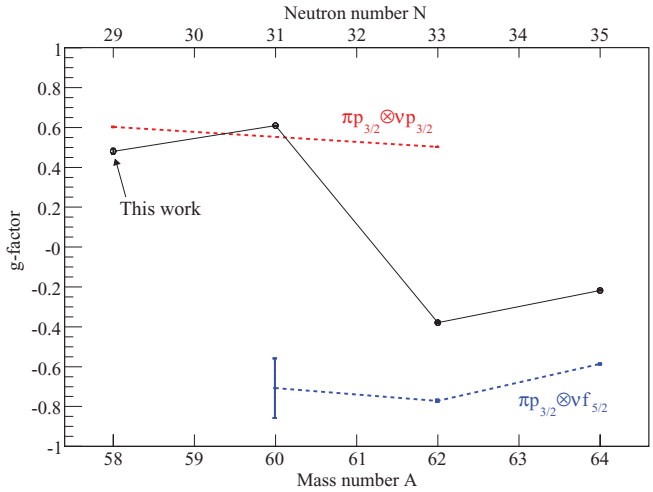

FIG. 9. (Color online) Systematic g factors of the 1^+, 2^+ state in odd-odd neutron-deficient copper isotopes. The colored dashed lines show the empirical g factors based on the additivity rule using the neighboring nickel (or zinc) and copper isotopes [29].

TABLE II. Isotope shift in GHz of the copper isotopes using the $3d^{10}4s\ ^2S_{1/2}$ to $3d^9 4s4p\ ^4P^\circ_{1/2}$ transition at 224.164 nm.

$^{57-63}$Cu	$^{58-63}$Cu	$^{59-65}$Cu	$^{63-65}$Cu
3.449(20)	3.137(180)	3.206(17)	0.977(21)

Using $I = 1$ for ^{58}Cu, a magnetic dipole moment $\mu(^{58}\text{Cu}) = +0.479(13)\mu_N$ is found. It is in reasonable agreement with the shell-model calculation using the GXPF1 interaction $0.60\mu_N$ [8,13] and with the Schmidt value $+0.627\mu_N$. The latter can be understood as the large discrepancy between the Schmidt value for the single proton [$\mu_S(\pi p_{3/2}) = +3.79\mu_N$, $\mu(^{57}\text{Cu}) = +2.582(7)\mu_N$] and for the single neutron [$\mu_S(\nu p_{3/2}) = -1.913\mu_N$, $\mu(^{57}\text{Ni}) = -0.7975(14)\mu_N$ [32]] cancel out.

The empirical moment can be calculated from the additivity of the g factors of ^{57}Ni (g_{Ni}) and ^{57}Cu (g_{Cu}) as [33]

$$\mu(^{58}\text{Cu}) = I_{58} \times \left[\frac{g_{\text{Cu}} + g_{\text{Ni}}}{2} + \frac{g_{\text{Cu}} - g_{\text{Ni}}}{2} \times \frac{I_{\text{Cu}}(I_{\text{Cu}}+1) - I_{\text{Ni}}(I_{\text{Ni}}+1)}{I_{58}(I_{58}+1)} \right]. \tag{7}$$

This equation can be greatly simplified since $I_{\text{Cu}} = I_{\text{Ni}} = I_{57} = \frac{3}{2}$. It becomes

$$\mu(^{58}\text{Cu}) = \frac{I_{58}}{I_{57}} \times \frac{\mu(^{57}\text{Cu}) + \mu(^{57}\text{Ni})}{2}, \tag{8}$$

where $\mu(^{57}\text{Cu}) = +2.582(7)\mu_N$ and $\mu(^{57}\text{Ni}) = -0.7975(14)\mu_n$ [32]. It gives a value of $+0.595(2)\mu_N$, also in reasonable agreement with our result.

Moreover, if one looks at the systematic of the g factors of the 1^+ and 2^+ states in the even-A copper isotopic chain, it can be seen that the additivity rule gives a qualitative indication of the purity of the proton-neutron configuration. Figure 9 compares the experimental g factors of the 1^+ and 2^+ neutron-deficient odd-odd copper isotopes to the empirical values. From this comparison, one can conclude that the $\pi p_{3/2} \otimes \nu p_{3/2}$ configuration dominates in the ground state of ^{58,60}Cu while it is the $\pi p_{3/2} \otimes \nu f_{5/2}$ configuration that dominates in the ground state of ^{62,64}Cu.

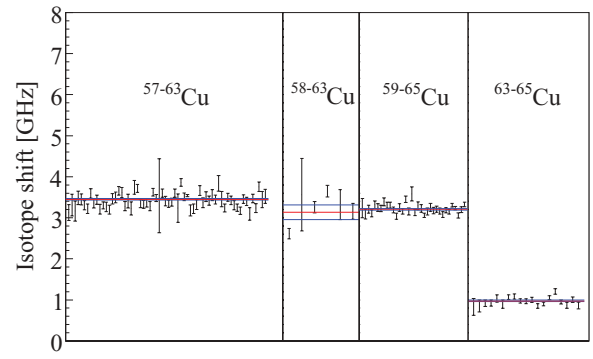

FIG. 10. (Color online) Systematic extracted isotope shift for the couples $^{57-63}$Cu, $^{58-63}$Cu, $^{59-65}$Cu, and $^{63-65}$Cu. The x axis represents the succession of experimental runs. The solid lines are the averages through the points.

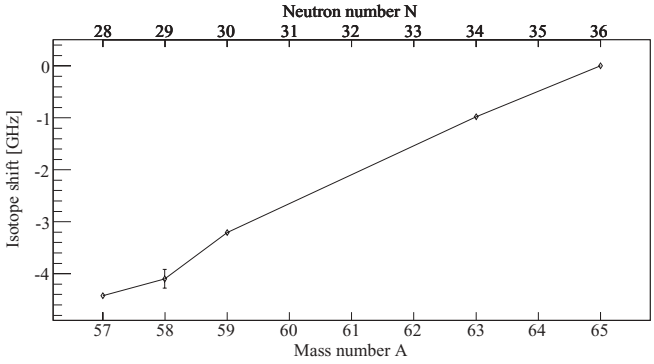

FIG. 11. Evolution of the isotope shift of copper in this work using the $3d^{10}4s\ ^2S_{1/2}$ to $3d^9 4s4p\ ^4P^\circ_{1/2}$ transition at 224.164 nm from $A = 57$ to $A = 65$.

C. Isotope shifts

Since two isotopes are always measured in parallel, the isotope shift can be extracted in each run free from the systematic drift discussed in the analysis of ^{63}Cu. The isotope shift is taken as the difference between the center of gravity of each hyperfine structure, extracted as described above. In that way, the isotope shift in the couples $^{57-63}$Cu, $^{58-63}$Cu, and $^{59-65}$Cu are extracted. In the case of $^{63-65}$Cu, an extrapolation of the drift of the center of gravity in ^{63}Cu is necessary. The drift is assumed to be linear in time in the course of the measurement of ^{65}Cu. Similarly to the hyperfine parameters, the isotope shift extracted for each run are shown in Fig. 10. The average values are given in Table II and shown in Fig. 11.

The isotope shifts between the four heaviest isotopes ^{58,59,63,65}Cu have been measured previously using a different transition ($3d^{10}4s\ ^2S_{1/2}$ to $3d^{10}4p\ ^2P_{1/2}$ at 327.4 nm [13,34]), allowing a comparison of the two transitions following the method of King [35]. The King plot is, however, not conclusive, due to the large contribution from the mass shift in the mass region of interest and the limited resolution of the in-source spectroscopy work, both here and in the work from Ref. [13]. No changes in the mean-square charge radius of copper can therefore be extracted.

IV. CONCLUSION

In-gas-cell resonant ionization laser spectroscopy has been performed for the first time at an online mass separator facility. The hyperfine structure of ^{57,58,59,63,65}Cu has been measured using for the first time the $^2S_{1/2}$ to $^4P^\circ_{1/2}$ transition at 224.164 nm. A systematic study of this transition on ^{63}Cu has shown that all systematic effects that can be attributed to the experimental setup cancel out in the data analysis. The magnetic dipole hyperfine parameter of the $3d^9 4s4p\ ^4P^\circ_{1/2}$ state has been measured for the first time in ^{57,59,63,65}Cu and its ratio to the ground-state magnetic dipole hyperfine parameter is 0.414(2). This is also the first laser spectroscopy measurement of the semimagic $N = 28$ isotope ^{57}Cu.

The magnetic dipole moments of ^{57,58,59,65}Cu are extracted based on that of ^{63}Cu. A new value of $+2.582(7)\mu_N$ is found for ^{57}Cu, in large disagreement with the previous literature value but in reasonable agreement with the shell-model calculations. A new value of $+0.479(13)\mu_N$ is presented for ^{58}Cu, in agreement with the previous literature value but more precise. The latter magnetic moment is consistent with a dominant $\pi p_{3/2} \otimes \nu p_{3/2}$ configuration, as expected in the vicinity of the closed-core nucleus ^{56}Ni. Although no direct confirmation of the spin assignment is possible with the studied transition, the nuclear spin of the different isotopes is strongly supported by this work, as any other spin assignment yields unphysical magnetic moments. Spins 0 for ^{58}Cu and $\frac{1}{2}$ for ^{57,59}Cu are firmly ruled out.

The isotope shifts between all five isotopes have been extracted. This mass region is however dominated by the mass shift and the resolution is insufficient to extract accurate information on the changes in the mean-square charge radii. Higher-precision in-source techniques, like the Laser Ion Source Trap (LIST) [36] coupled to a gas cell [21] or the use of two-photon excitation or saturation spectroscopy [37] in a hot cavity, would yield the required accuracy for that type of study while maintaining the high sensitivity.

ACKNOWLEDGMENTS

Fruitful discussions with G. Neyens and N. Severijns are greatfully acknowledged. We thank the CRC team, Louvain-La-Neuve (Belgium), for providing the primary beams. This work was supported by FWO-Vlaanderen (Belgium), GOA/2004/03 (BOF-K.U.Leuven), the IUAP-Belgian State-Belgian Science Policy-(BriX network P6/23), and by the European Commission within the Sixth Framework Programme through I3-EURONS (Contract RII3-CT-2004-506065).

[1] B. Bastin, S. Grévy, D. Sohler, O. Sorlin, Zs. Dombrádi, N. L. Achouri, J. C. Angélique, F. Azaiez, D. Baiborodin, R. Borcea *et al.*, Phys. Rev. Lett. **99**, 022503 (2007).

[2] L. Gaudefroy, J. M. Daugas, M. Hass, S. Grévy, Ch. Stodel, J.-C. Thomas, L. Perrot, M. Girod, B. Rossé, J. C. Angélique *et al.*, Phys. Rev. Lett. **102**, 092501 (2009).

[3] K. L. Yurkewicz, D. Bazin, B. A. Brown, C. M. Campbell, J. A. Church, D. C. Dinca, A. Gade, T. Glasmacher, M. Honma, T. Mizusaki *et al.*, Phys. Rev. C **70**, 054319 (2004).

[4] O. Perru, O. Sorlin, S. Franchoo, F. Azaiez, E. Bouchez, C. Bourgeois, A. Chatillon, J. M. Daugas, Z. Dlouhy, Zs. Dombrádi *et al.*, Phys. Rev. Lett. **96**, 232501 (2006).

[5] G. Audi, A. H. Wapstra, and C. Thibault, Nucl. Phys. **A729**, 337 (2003).

[6] G. Kraus, P. Egelhof, C. Fischer, H. Geissel, A. Himmler, F. Nickel, G. Müzenberg, W. Schwab, A. Weiss, J. Friese *et al.*, Phys. Rev. Lett. **73**, 1773 (1994).

[7] A. F. Lisetskiy, N. Pietralla, M. Honma, A. Schmidt, I. Schneider, A. Gade, P. von Bretano, T. Otsuka, T. Mizusaki, and B. A. Brown, Phys. Rev. C **68**, 034316 (2003).
[8] M. Honma, T. Otsuka, B. A. Brown, and T. Mizusaki, Phys. Rev. C **69**, 034335 (2004).
[9] J. Rikovska, T. Giles, N. J. Stone, K. van Esbroeck, G. White, A. Wöhr, M. Veskovic, I. S. Towner, P. F. Mantica, J. I. Prisciandaro *et al.*, Phys. Rev. Lett. **85**, 1392 (2000).
[10] L. Weissman, U. Köster, R. Catherall, S. Franchoo, U. Georg, O. Jonsson, V. N. Fedoseyev, V. I. Mishin, M. D. Seliverstov, J. Van Roosbroeck *et al.*, Phys. Rev. C **65**, 024315 (2002).
[11] V. V. Golovko, I. Kraev, T. Phalet, N. Severijns, B. Delauré, M. Beck, V. Kozlov, A. Lindroth, S. Versyck, D. Zákoucký *et al.*, Phys. Rev. C **70**, 014312 (2004).
[12] K. Minamisono, P. F. Mantica, T. J. Mertzimekis, A. D. Davies, M. Hass, J. Pereira, J. S. Pinter, W. F. Rogers, J. B. Stoker, B. Tomlin *et al.*, Phys. Rev. Lett. **96**, 102501 (2006).
[13] N. J. Stone, U. Köster, J. R. Stone, D. V. Fedorov, V. N. Fedoseyev, K. T. Flanagan, M. Hass, and S. Lakshmi, Phys. Rev. C **77**, 067302 (2008).
[14] N. J. Stone, K. Van Esbroeck, J. Rikovska Stone, M. Honma, T. Giles, M. Veskovic, G. White, A. Wöhr, V. I. Mishin, V. N. Fedoseyev *et al.*, Phys. Rev. C **77**, 014315 (2008).
[15] T. E. Cocolios, A. N. Andreyev, B. Bastin, N. Bree, J. Büscher, J. Elseviers, J. Gentens, M. Huyse, Yu. Kudryavtsev, D. Pauwels *et al.*, Phys. Rev. Lett. **103**, 102501 (2009).
[16] K. T. Flanagan, P. Vingerhoets, M. Avgoulea, J. Billowes, M. L. Bissell, K. Blaum, B. Cheal, M. De Rydt, V. N. Fedosseev, D. H. Forest *et al.*, Phys. Rev. Lett. **103**, 142501 (2009).
[17] S. Büttgenbach, Hyperfine Interact. **20**, 1 (1984).
[18] K. Flanagan, ISOLDE Newsletter, p. 11 (2009).
[19] M. D. Seliverstov, A. E. Barzakh, I. Ya. Chubukov, D. V. Fedorov, V. N. Panteleev, and Yu. M. Volkov, Hyperfine Interact. **127**, 425 (2004).
[20] J. Lettry, R. Catherall, P. Drumm, P. Van Duppen, A. H. M. Evensen, G. J. Focker, A. Jokinen, O. C. Jonsson, E. Kugler, and H. Ravn, Nucl. Instrum. Methods B **126**, 130 (1997).
[21] T. Sonoda, T. E. Cocolios, J. Gentens, M. Huyse, O. Ivanov, Yu. Kudryavtsev, D. Pauwels, P. Van den Bergh, and P. Van Duppen, Nucl. Instrum. Methods B **267**, 2918 (2009).
[22] Yu. Kudryavtsev, T. E. Cocolios, J. Gentens, M. Huyse, O. Ivanov, D. Pauwels, T. Sonoda, P. Van den Bergh, and P. Van Duppen, Nucl. Instrum. Methods B **267**, 2908 (2009).
[23] Yu. Kudryavtsev, B. Bruyneel, J. Gentens, M. Huyse, P. Van den Bergh, P. Van Duppen, and L. Vermeeren, Nucl. Instrum. Methods B **179**, 412 (2001).
[24] D. Pauwels, O. Ivanov, J. Büscher, T. E. Cocolios, J. Gentens, M. Huyse, A. Korgul, Yu. Kudryavtsev, R. Raabe, M. Sawicka *et al.*, Nucl. Instrum. Methods B **266**, 4600 (2008).
[25] Yu. Kudryavtsev, J. Andrzejewski, B. Bijnens, S. Franchoo, J. Gentens, M. Huyse, A. Piechaczek, J. Szerypo, I. Reusen, P. Van den Bergh *et al.*, Nucl. Instrum. Methods B **114**, 350 (1996).
[26] S. Gheysen, G. Neyens, and J. Odeurs, Phys. Rev. C **69**, 064310 (2004).
[27] H. Figger, D. Schmitt, and S. Penselin, Coll. int. du CNRS **164**, 355 (1967).
[28] O. Lutz, H. Oehler, and P. Kroneck, Z. Phys. A **288**, 17 (1978).
[29] N. J. Stone, At. Data Nucl. Data Tables **90**, 75 (2005).
[30] P. R. Locher, Phys. Rev. B **10**, 801 (1974).
[31] D. R. Semon, M. C. Allen, H. Dejbakhsh, C. A. Gagliardi, S. E. Hale, J. Jiang, L. Trache, R. E. Tribble, S. J. Yennello, H. M. Xu *et al.*, Phys. Rev. C **53**, 96 (1996).
[32] T. Ohtsubo, D. J. Cho, Y. Yanagihashi, S. Ohya, and S. Muto, Phys. Rev. C **54**, 554 (1996).
[33] P. C. Zalm, J. F. A. van Hienen, and P. W. M. Glaudemans, Z. Phys. A **287**, 255 (1978).
[34] G. Hermann, G. Lasnitschka, C. Schwabe, and D. Spengler, Spectrochimica Acta **48B**, 1259 (1993).
[35] W. H. King, *Isotope Shift in Atomic Spectra* (Plenum Press, New York, 1984).
[36] K. Blaum, C. Geppert, H.-J. Kluge, M. Mukherjee, S. Schwarz, and K. Wendt, Nucl. Instrum. Methods B **204**, 331 (2003).
[37] V. P. Denisov, Nucl. Instrum. Methods A **345**, 99 (1994).